Determinants of tidal recruitment/derecruitment assessed by electrical impedance tomography in spontaneously breathing ARDS patients

Joaquin Perez[5,6], Marco Leali[1], Elena Spinelli[2], Valentina Chiavieri[1], Tommaso Rosà[3,4], Pierluigi Ferrara[7,8], Gaetano Scaramuzzo[7,8], Massimo Antonelli[3,4], Giacomo Grasselli[1,2], Domenico L. Grieco[3,4], Savino Spadaro[7,8] Tommaso Mauri[1,2].

1. Department of Pathophysiology and Transplantation, University of Milan, Milan, Italy.
2. Department of Anesthesia, Critical Care and Emergency, Fondazione IRCCS Ca' Granda Maggiore Policlinico Hospital, Milan, Italy.
3. Department of Emergency, Intensive Care Medicine and Anesthesia, Fondazione Policlinico Universitario A. Gemelli IRCCS, Rome, Italy.
4. Department of Anesthesiology and Intensive Care Medicine, Catholic University of the Sacred Heart, Rome, Italy.
5. Department of Physical Therapy and Rehabilitation, Anchorena San Martín Clinic, Buenos Aires, Argentina.
6. Department of Emergency Medicine, Carlos G. Durand Hospital, Buenos Aires, Argentina
7. Department of Translational Medicine, University of Ferrara, Sant'Anna Hospital, Ferrara, Italy.
8. Department of Emergency Medicine, Intensive care Unit, Azienda Ospedaliera Universitaria di Ferrara, Ferrara, Italy.

Corresponding author

Prof. Tommaso Mauri

Department of Pathophysiology and Transplantation, University of Milan, Milan, Italy

Via F. Sforza 35, 20122 Milan, Italy

E-mail: tommaso.mauri@unimi.it

Author's contributions to the study: Substantial contributions to the conception or design of the work: JP, ML and TM. Acquisition, analysis, or interpretation of data for the work: all authors. Drafting the work or revising it critically for important intellectual content: all authors. Final approval of the version submitted for publication: all authors. Accountability for all aspects of the work in ensuring that questions related to the accuracy or integrity of any part of the work are appropriately investigated and resolved: all authors.

Sources of support: Institutional funding of the Department of Anesthesia, Critical Care and Emergency, Fondazione IRCCS Ca' Granda Ospedale Maggiore Policlinico, Milan, Italy; Current research, Italian Ministry of Health, Rome, Italy; Project "Hub Life Science - Diagnostica Avanzata (HLS-DA), PNC-E3-2022-23683266– CUP: C43C22001630001 / MI-0117", Italian Ministry of Health, Rome, Italy (Piano Nazionale Complementare Ecosistema Innovativo della Salute); The Italian Ministry of Education and Research (MUR), Rome Italy: Dipartimenti di Eccellenza Program 2023–2027 - Dept. of Pathophysiology and Transplantation, University of Milan.

Running head: Tidal recruitment/derecruitment assessed with EIT on PSV

Descriptor number: 4.8 Mechanical Ventilation: Physiology & Pathophysiology

Total word count: 3713 words

This article has an online data supplement, which is accessible from this issue's table of content online at **www.atsjournals.org**

Artificial Intelligence Disclaimer: No artificial intelligence tools were used in writing this manuscript.

Abstract

Word count: 265

Rationale: Tidal recruitment/derecruitment (R/D) is a well-known mechanism of lung injury in ARDS patients, but its bedside identification is challenging during assisted ventilation.

Objectives: To investigate bedside determinants of tidal R/D assessed by electrical impedance tomography (EIT) in spontaneously breathing ARDS patients on pressure support ventilation (PSV).

Methods: Secondary analysis of a previous study including lightly sedated ARDS patients ventilated on PSV at two PEEP levels selected by EIT ($PEEP_{EIT}$) and low PEEP/FiO_2 table ($PEEP_{TABLE}$). Detailed physiological assessment was performed, including respiratory mechanics, inspiratory drive and effort, regional mechanics and tidal R/D measured by EIT.

Measurements and Main Results: Of 30 original patients, one was excluded due to unstable end-expiratory lung impedance, leaving 29 patients for analysis. Median PEEP was 10.0 [8.0-12.0] cmH_2O with $PEEP_{EIT}$ and 8.0 [5.0-10.0] cmH_2O with $PEEP_{TABLE}$. Overall, tidal R/D was 14.3% [9.0–33.0], but it was lower at $PEEP_{EIT}$ vs. $PEEP_{TABLE}$ (11.3% [4.8–20.5] vs. 21.9% [6.8–31.7]; P=0.008). R/D reduction with $PEEP_{EIT}$ correlated with decreases in collapse (rho=0.72; P<0.001) and pendelluft (rho=0.57; P=0.002).

Analyzing data from both randomized PEEP together, mixed-effects models showed higher tidal R/D at lower PEEP (P<0.001), more negative end-expiratory transpulmonary pressure ($PL_{End\text{-}Exp}$) (P<0.001), larger collapse (P<0.001) and lower lung compliance (P=0.002). Higher respiratory drive (P=0.001), effort (P=0.009), and dynamic driving transpulmonary pressure (P=0.009) correlated with higher tidal R/D. Patients with non-focal infiltrates presented higher tidal R/D (P=0.005).

At multivariable analysis, $PL_{End\text{-}Exp}$, lung collapse and non-focal pattern were independently associated tidal R/D.

Conclusion: In spontaneously breathing ARDS patients on PSV, the main determinants of tidal R/D are more negative $PL_{End\text{-}Exp}$, higher lung collapse and non-focal infiltrates.

Key words: Electrical impedance tomography, physiologic monitoring, assisted ventilation, acute respiratory distress syndrome, ventilator-induced lung injury

Introduction

Cyclic alveolar recruitment/derecruitment (R/D) induced by tidal ventilation is a well-known mechanism of lung injury (atelectrauma)(1,2). Multiple studies have shown that repetitive opening and closing of distal airways may intensify the frictional and compressive forces exerted on the lung epithelial surface(2–6), which disrupts the alveolar-capillary barrier and impairs surfactant function, contributing to pulmonary edema, inflammation, and hyaline membranes formation(2,7–10).

Measuring tidal R/D at the bedside is challenging, particularly in spontaneously breathing patients at risk for patient self-inflicted lung injury (P-SILI). A recent experimental study described a novel method to measure tidal R/D at the bedside by electrical impedance tomography (EIT)(11). Nevertheless, this approach has not yet been applied in patients with the acute respiratory distress syndrome (ARDS) spontaneously breathing at different positive end-expiratory pressure (PEEP) levels. In this context, tidal R/D can be influenced by multiple mechanisms, including respiratory effort, lung stress and the effect of PEEP on alveolar recruitment. Bedside detection of tidal R/D might add relevant information for a safer transition from controlled to assisted ventilation(12,13).

In this study, we examined the physiological and clinical determinants of tidal R/D assessed by EIT in intubated patients with ARDS undergoing pressure support ventilation (PSV) at different PEEP levels. Some of these results have been previously reported in the form of an abstract(14).

Methods

Study design

This study is a secondary analysis of a randomized, crossover trial carried out in 3 Italian ICUs that compared the effects of two personalized PEEP levels on lung and diaphragm protection(15). One method assigned PEEP according to the lower PEEP/FiO_2 table ($PEEP_{TABLE}$), while the other selected the PEEP associated with lowest absolute difference between alveolar collapse and overdistension measured by EIT and driving transpulmonary pressure ($PEEP_{EIT}$).

Population

The original study enrolled adults with ARDS and Richmond Agitation-Sedation Score between -2 and 0 ventilated on PSV as per clinical decision. Exclusion criteria were clinical $FiO_2 > 0.8$, age < 18 years, hemodynamic instability, pneumothorax, history of severe obstructive pulmonary disease, inability to correctly position the EIT belt, contraindications to EIT monitoring or to esophageal catheter insertion. For the present study, one of the thirty patients originally enrolled was excluded because of unstable end-expiratory lung impedance (EELI) values.

Data collection

At inclusion, we collected demographic data, Simplified Acute Physiology Score II (SAPS II) at ICU admission, Sequential Organ Failure Assessment (SOFA) score, days from intubation, days since PSV transition, etiology of ARDS, sedation and analgesia, ventilator settings, and blood gases. Focal and non-focal lung morphology – assessed through chest computed tomography (CT) (n=16) or chest radiography (n=13) – was classified by two independent reviewers (M.L, V.C) with disagreement resolved by consensus. Patient outcomes were collected from electronic clinical records.

Measurements

Esophageal pressure (P_{es}) was monitored by a dedicated catheter (Cooper Surgical, CT, USA or Nutrivent, Sidam, Italy) inflated according to manufacturer's recommendations. The correct positioning of the balloon was checked(16). Airway and esophageal pressure (P_{aw} and P_{es}) were continuously monitored by a dedicated system (PulmoVista 500, Drager, Lübeck, Germany) and transpulmonary pressure (PL) was calculated as the difference between P_{aw} and P_{es}. Dynamic driving PL (ΔPL_{dyn}) was computed as the difference between the maximal and minimal PL. The airway occlusion pressure at 100 ms ($P_{0.1}$) and occlusion pressure (ΔP_{occ}) were measured during an occluded airway at the end of expiration.

EIT monitoring was performed using a dedicated belt with 16 electrodes connected to the EIT monitor (PulmoVista® 500, Drager, Lübeck, Germany). EIT data were acquired at a frame rate of 50 Hz and stored for offline analysis.

Study protocol

The original study consisted of 3 phases: first, all patients underwent a decremental PEEP trial from 18 to 4 cmH_2O in supine semi-recumbent position, with 2-cmH_2O steps lasting 2 minutes (*phase-1*). After the decremental trial, two PEEP levels were identified ($PEEP_{TABLE}$ and $PEEP_{EIT}$). Then, patients were ventilated for 20 min at each PEEP level in randomized order (*phase-2 and 3*).

During the decremental PEEP trial and the last minutes of each randomized PEEP, a detailed physiological assessment was performed including respiratory parameters, EIT ventilation data, gas exchange (only for *phase-2* and *3*) and hemodynamics (*see* **Supplementary material**). Throughout all the study, analgesia and sedation dose were kept constant.

Quantification of tidal recruitment/derecruitment using EIT

EIT recordings within the same patient were reconstructed against the same baseline end-expiratory frames at the lowest PEEP level evaluated during the decremental trial (*phase1*, 4 cmH_2O step) (Draeger's proprietary algorithm software version 1.3).

Then, the analysis for tidal R/D was performed as follows: towards the end of each 20 min randomized PEEP level (*phase-2 and 3*), we visually selected a stable period comprising 13 [10–18] breaths to reconstruct EIT maps at end-inspiration and end-expiration. By subtraction of the end-inspiratory and end-expiratory maps, tidal breathing images were derived.

We then identified tidal R/D as previously described(11): at end-expiration, pixels were classified as "aerated" if the increase of EELI from PEEP 4 cmH_2O to the target PEEP level ($PEEP_{EIT}$ and $PEEP_{TABLE}$) was >10% of the maximal change. Pixels were classified as "ventilated" if their tidal impedance variation exceeded 30% of the maximal value within that tidal image. A detailed explanation for the selected ventilation/aeration thresholds and a sensitivity analysis of the main results is presented in **Supplementary material.**

A pixel was classified as undergoing tidal R/D if "non-aerated" at end-expiration but "ventilated" in the tidal breathing image (**Figure 1**). The percentage of tidal R/D at each PEEP level was computed as:

$$\text{Tidal recruitment/derecruitment}_{\%} = \left(\frac{\Sigma \text{ Pixels ventilated AND non-aerated (randomized PEEP level)}}{\Sigma \text{ Pixels aerated OR ventilated (PEEP 18 cmH}_2\text{O)}}\right) \text{ x } 100$$

Given that tidal R/D is often expressed as a fraction of the total lung volume or lung weight(17), pixels aerated or ventilated in EIT images obtained at the highest PEEP during the decremental trial (*phase-1*, PEEP 18 cmH_2O) were used as denominator in

the formula, as this PEEP was the closest available proxy to the maximal total lung aeration in our study.

Regional values of tidal R/D were analyzed within 3 horizontal regions of interest (ROIs) from ventral to dorsal: non-dependent (11x32), middle (10x32) and dependent (11x32)

Statistical Analysis

Data are expressed as mean ± standard deviation or median [1st–3rd quartile], according to Shapiro–Wilk test results. Categorical variables are presented as number (percentage). The comparison between tidal R/D at $PEEP_{EIT}$ and $PEEP_{TABLE}$ was performed with linear mixed-effects models including patient as a random intercept accounting for the hierarchical and dependent structure of data. Correlations between non-repeated measures were assessed through Spearman coefficient (ρ).

Bivariate associations were explored through mixed-effects models using data from both randomized PEEP were together (2 points per patient). Patients were entered as random intercepts and slopes. Effect estimates are reported as beta coefficients (β) with 95% confidence intervals (CI). When the dependent variable required transformation to satisfy model assumptions, coefficients were reported on the transformed scale. The variance explained by fixed effects alone and by the full model (including random effects) was quantified using marginal (R^2_m) and conditional (R^2_c) determination coefficient, respectively(18).

Independent determinants of tidal R/D were evaluated using multivariable linear mixed-effects modeling. A primary multivariable mixed-effects model was constructed with variables selected a priori based on physiological relevance and prior evidence. These included the following parameters treated as numerical continuous predictors: tidal volume adjusted to predicted body weight (Vt/PBW), PEEP, muscular pressure (P_{mus}), ΔPL_{dyn}, pendelluft, and reversible lung collapse(19–24). To address potential

confounding, baseline radiological pattern based on pulmonary infiltrates distribution (treated as categorical variable, focal vs. non-focal) and baseline respiratory system compliance (treated as numerical continuous variable) were also incorporated as fixed effects. A backward stepwise selection was applied to the primary model to reduce complexity and mitigate overfitting and variables with P<0.15 were retained (**Table E2**)(25). The final reduced model was refitted to identify independent determinants of tidal R/D. Additionally, coefficients of continuous numerical variables were standardized to compare the relative magnitude of the effect of each variable on tidal R/D (*see* supplementary material).

We performed additional exploratory analysis. We evaluated the ability of the end-expiratory PL ($PL_{End-Exp}$), airway occlusion pressure at 100 ms ($P_{0.1}$), P_{mus}, and ΔPL_{dyn} to identify risk of atelectrauma (defined as tidal R/D ≥10.0%) through receiver operator curves (ROC) derived from generalized binomial mixed models, incorporating patient-specific random effects(26–28). The area under the curve (AUC) of each predictor was obtained from the marginal predictions derived from fixed effects. To improve clinical interpretation, we assessed the discriminative power of different clinical cutoffs for each of variable. Sensitivity, specificity, area under the curve and Youden index of each cutoff are reported. We also repeated the analysis using alternative tidal R/D percentages (5%, 14.3%, and 20%) to classify patients at risk.

Finally, the predicted probability of hospital discharge and weaning was assessed using cox regression model, adjusted by age and clinical PEEP level, stratifying patients into high and low tidal R/D groups. For this analysis, tidal R/D values measured at each randomized PEEP were averaged per patient, and the population was dichotomized into high tidal R/D group (≥14.3%) or low tidal R/D group (<14.3%) based on the median value.

A two-tailed P-value <0.05 was deemed statistically significant (R software version 4.2.2).

Results

Study population

We included twenty-nine patients (**Table 1**). The patients were 64.0±14.0 years and most of them had primary ARDS (n=22; 75.8%) and non-focal distribution of pulmonary infiltrates (n=17; 58.6%). At inclusion, patients had been intubated for 6.0 [3.5–9.5] days and had spent 3.0 [1.0–5.0] days on PSV. The mean clinical pressure support (PS) level was 9.0±2.0 cmH_2O, PEEP was 9.2±3.0 cmH_2O and FiO_2 0.45 [0.40–0.50]. PaO_2/FiO_2 was 206±54 and $PaCO_2$ was 45±6.3 mmHg.

During the randomized study phases, the median PEEP assigned at $PEEP_{EIT}$ and $PEEP_{TABLE}$ was 10.0 [8.0-12.0] cmH_2O and 8.0 [5.0-10.0] cmH_2O, respectively. Additional parameters collected during the two randomized PEEP levels are detailed in **Table S1**.

Localization and quantification of tidal recruitment / derecruitment

As illustrated in **Figure 1**, most of tidal R/D occurred in the middle and dorsal parts of the lungs. This regional distribution remained consistent both during $PEEP_{EIT}$ and $PEEP_{TABLE}$ phase (**Figure E2**).

Analyzing data from both randomized PEEP levels together, the median tidal R/D was 14.3% [5.1–27.7]. Tidal R/D magnitude was lower when PEEP was set according to EIT method versus $PEEP/FiO_2$ table (11.3% [4.8–20.5] vs. 21.9% [6.8–31.7]; P=0.008) (**Figure 2**). The reduction of tidal R/D when the assigned PEEP level was changed from $PEEP_{TABLE}$ to $PEEP_{EIT}$ correlated with decreases in pendelluft and lung collapse (**Figure E2**).

Variables associated with tidal recruitment/derecruitment

Table 2 summarizes the bivariate unadjusted associations between tidal R/D, ventilator settings, monitoring and patients baseline characteristic, based on mixed-effects models combining data from $PEEP_{EIT}$ and $PEEP_{TABLE}$.

- *End-expiratory lung inflation and lung compliance*

Ventilation at lower PEEP levels and more negative $PL_{End\text{-}Exp}$ led to higher fractions of tidal R/D (**Figure 3A**). Higher tidal R/D also correlated with larger amount of reversible lung collapse (**Figure 3B**), and lower dynamic lung compliance (CL_{dyn}), but it was was better associated with collapse localized in the dependent regions (i.e., dorsal CL_{dyn}) than with non-dependent collapse (**Figure E3**).

- *Respiratory drive, effort and lung stress*

Higher respiratory drive ($P_{0.1}$) correlated with more tidal R/D (**Figure E4**). Similarly, stronger inspiratory effort (P_{mus}, ΔP_{es}, and ΔP_{occ}) and work of breathing (PTP_{mus} per minute) correlated with increased tidal R/D (**Figure E5**). Higher elastic end-inspiratory pressure was associated with a reduction of tidal R/D, likely because changes in end-inspiratory pressure followed increase of end-expiratory pressure (**Figure E6**): tidal R/D decreased at increasing plateau pressure but this association was stronger with higher static $PL_{End\text{-}Insp}$ (**Figure E7**). Tidal R/D also increased with higher dynamic lung stress (ΔPL_{dyn} and ΔPL_{stat}) but this association was not related to the set PS level. In fact, a greater contribution of respiratory effort to the total dynamic lung stress (i.e., $\Delta P_{es}/\Delta PL_{dyn}$ relationship) led to larger tidal R/D. The difference between ΔPL_{dyn} and ΔPL_{stat}—a variable suggested to reflect heterogeneity of lung stress distribution across dependent and non-dependent regions (22,30)—positively correlated with tidal R/D.

- *Ventilation heterogeneity and breathing pattern*

Increased tidal R/D was associated with more heterogeneous intrapulmonary distribution of ventilation (global and local inhomogeneity index). No association was found between pendelluft and tidal R/D. Classical breathing patterns parameters, including Vt/PBW, respiratory rate, and I:E ratio, showed no association with tidal R/D (**Figure E8**).

- *Baseline patients characteristics*

Patients with non-focal distribution of pulmonary infiltrates (n=17) showed significantly higher values of tidal R/D compared with those with focal lung morphology (n=12) (**Figure 3C**). The remaining patients characteristics were not associated with tidal R/D (**Table 2**).

Independent determinants of tidal recruitment / derecruitment

- *Adjusted multivariable analysis*

After applying the stepwise backward regression to the full primary model, the variables retained in the final model as independent determinants of tidal R/D were $PL_{End-Exp}$, reversible lung collapse, ΔPL_{dyn} and lung morphology **(Table E3**).

In the final model, $PL_{End-Exp}$ (coefficient -0.12 [95% CI, -0.22 – -0.02]), reversible lung collapse (coefficient 0.07 [95% CI, 0.03 – 1.10]) and morphological distribution of lung infiltrates (coefficient 1.49 [95% CI, 0.61 – 2.36]) exerted independent effect on tidal R/D whereas ΔPL_{dyn} did not (coefficient 0.06 [95% CI, -0.06 – 0.14]) (**Table 3**).

When coefficients of the three numerical continuous variables ($PL_{End-Exp}$, lung collapse and ΔPL_{dyn}) were standardized to allow comparison, reversible collapse exerted the largest effect on tidal R/D (**Figure 4).**

Exploratory outcomes

Respiratory monitoring to detect atelectrauma risk

The discriminative performance of different clinical cutoffs of bedside monitoring variables for identifying patients at risk of atelectrauma (defined as a tidal R/D ≥10%) is summarized in **Table 4**. Overall, the ROC curves demonstrated a reasonable predictive capacity, with $PL_{End-Exp}$ and $P_{0.1}$ showing the strongest diagnostic performance. Additional

analyses using alternative tidal R/D thresholds (≥5%, ≥14.3%, and ≥20%) to define atelectrauma risk are presented in **Table E5**.

Tidal recruitment / derecruitment and clinical outcomes

Patients in the *high tidal R/D* group (n=14) – i.e., those with a mean tidal R/D ≥14.3% calculated as the average of R/D values observed at $PEEP_{EIT}$ and $PEEP_{TABLE}$ – had a median magnitude of tidal R/D of 27.7% [20.8–35.3]. The *low tidal R/D* group (n=15) exhibited a median value of tidal R/D of 5.6% [2.0–11.3].

After adjusting for age and PEEP level at enrollment, the cox regression models showed that patients in the *high tidal R/D* group had lower probabilities of being weaned from MV (hazard ratio: 0.39 [95% CI, 0.19–0.80]; P=0.011) **(Figure E9)** and discharged alive from the hospital (hazard ratio: 0.37 [95% CI, 0.18–0.76]; P=0.006) (**Figure 5)** compared with patients in the *low tidal R/D* group.

Discussion

This study describes key physiological determinants of tidal R/D assessed through EIT in ARDS patients undergoing assisted ventilation. Our main findings are: 1) tidal R/D magnitude seems clinically relevant but highly variable among patients; 2) higher respiratory drive, effort and dynamic lung stress increased tidal R/D, but this associations did not remain significant after adjustment by confounders; 3) instead, the main physiological determinants of higher tidal R/D were higher reversible lung collapse, more negative $PL_{End\text{-}Exp}$ and non-focal lung morphology; 4) patients with higher tidal R/D exhibited lower chances of hospital discharge and weaning.

The pathophysiological implications of tidal R/D have been known for decades(4, 10, 30–34). Yet the physiology of tidal R/D in critically ill patients remain scarcely characterized during assisted ventilation, largely due to the technical challenges in measuring it. The bedside, dynamic, noninvasive and radiation-free nature of EIT may offer advantages over other less feasible monitoring(3,34,36–39).

Of note, the observed values of tidal R/D are higher than those previously reported. Liu et al.(11) reported R/D ~10% assessed by EIT in ARDS models during controlled ventilation. Nonetheless, the dynamics of tidal R/D may vary widely with the presence of respiratory effort. According to the solid-like behavior, pressure changes during SB are concentrated in the dependent-middle lung regions, where more collapse is found and most tidal R/D occurs(20). Contrarily, during passive ventilation, positive pressure is predominantly applied on the non-dependent baby lung, where collapse and tidal R/D are minimal(39). In fact, tidal R/D was mainly driven by respiratory effort rather than by the pressure support in the bivariate analysis. In another study, tidal R/D ranged from 6% to 16%, as measured by dynamic CT(19). Importantly, $PL_{End\text{-}exp}$ was highly positive in that study (+4.2 cmH_2O and +4.8 cmH_2O in mild and severe ARDS animal models), compared with values as negative as -10 to -5 cmH_2O in some of our patients. Furthermore, animals had considerably lower effort (ΔPes: 0.4–6 cmH_2O) than the patients enrolled in our study (ΔPes: 3–17 cmH_2O). Interestingly, it has been observed that tidal R/D values may be close to those observed in our cohort (~15%) when $PL_{End\text{-}exp}$ is clearly negative(17).

In highly recruitable ARDS models, Yoshida et al. observed that excessive respiratory effort aggravated lung injury partly mediated by tidal R/D(19). We showed a positive association of respiratory drive, effort and lung stress with tidal R/D, but this correlation did not remain independent after adjustments. Physiologically, tidal R/D is feasible at increasing lung distending pressures even in mild ARDS(40). Nonetheless, tidal R/D is expected to occur only when three conditions present simultaneously: 1) regional $PL_{End\text{-}exp}$ lower than alveolar closing pressure, leading to expiratory collapse; 2) potential for lung recruitment during inspiration; 3) inspiratory transalveolar pressure (alveolar – pleural pressure) higher than alveolar opening pressure.

Contrary to our findings, previous studies have reported that Vt is a central determinant of cyclic R/D(25,39). This association is reasonable, however, when different Vt are compared under the same PEEP level. Halter et al. observed that

increasing Vt from 6 to 12 ml/kg did not increase tidal R/D when PEEP was contemporarily increased from 5 to 10 cmH_2O(38). In our study, PEEP was actively modified, and changes in Vt were largely secondary to PEEP-induced changes in lung compliance. Under these conditions, lower tidal R/D may occur despite higher Vt, because increased PEEP reduces expiratory derecruitment while simultaneously improving compliance, thereby allowing patients to breathe at higher Vt. Furthermore, Vt was within protective limits in most of the cases, precluding us from exploring the impact of more extreme Vt on tidal R/D.

Although pendelluft magnitude was not independently associated with tidal R/D in our study population, the reduction of pendelluft did correlate with lower tidal R/D when PEEP was adjusted according the $PEEP_{EIT}$ strategy. This response was mainly observed in patients where $PEEP_{EIT}$ assigned higher PEEP and reduced lung collapse. This is consistent with findings reported by Morais et al., in which higher PEEP appropriately selected in more recruitable patients reduced lung collapse, and decreased pendelluft and tidal R/D(23). Also, these results suggest that changes in pendelluft – rather than its absolute value – when PEEP levels are modified may be more physiologically informative depending on the effects of PEEP on respiratory mechanics. The lack of a baseline association may be explained by the presence of other phenomena beyond reopening of collapse regions contributing to regional gas dyssynchrony and pendelluft specially at low PEEP levels (such as increased distal resistance)(41).

One of our most physiologically sound results is close association between more negative values of $PL_{End\text{-}Exp}$, higher reversible lung collapse and tidal R/D. Notably, correlations between $PL_{End\text{-}Exp}$, collapse and tidal R/D were independent from PEEP settings, underscoring the need to appropriately target PEEP during assisted ventilation to counterbalance pleural and superimposed pressures that lead to alveolar collapse(36,37,42).

Caironi et al.(36) previously reported that tidal R/D was relevant only in patients with diffuse infiltrates distribution. Similarly, we observed that patients with non-focal

ARDS had significantly higher tidal R/D, with may potentially inform in the future about the decision to switch ARDS patients to assisted ventilation. While tidal R/D could be detected by lung hysteresis during controlled ventilation(43,44), EIT may be necessary to identify it during assisted spontaneous breathing.

Tidal R/D seems a potential predictor of outcome, likely because the mean value between the two randomized phases conflates a mix of disease severity, treatment response and risk of additional injury by ventilation. However, these results must be interpreted with great caution because of the physiological nature of our study. Also, the small sample size precluded us from adjusting for other potential confounders. Additionally, other factors such as PEEP settings in the following days could have modify the patient's trajectories and influenced outcome. These findings provide a rationale and conceptual framework for future interventional studies designed to determine whether strategies such as adjusting PEEP to reduce tidal R/D are associated with improved clinical outcomes

Limitations

First, we did not validate of our EIT-based measure of tidal R/D with a reference technique (e.g. CT-scan). This would have been clinically unpracticable considering the associated risks of exposing patients to those interventions. Albeit preliminary and hypothesis-generating, our findings are supported by a strong physiological rational, which encourage further investigation and warrant confirmation in future research. Second, the thresholds selected to define ventilation and aeration were empirical. For this reason, we performed multiple sensitivity analysis combining different thresholds to describe how this selection modified the analysis. Future studies should evaluate how different thresholds correlate with a gold standard technique to define which aeration/ventilation combination must be adopted in future investigation. Third, our cohort included patients in the recovering phase of ARDS. Although tidal R/D could be even more relevant in earlier stages, the results may not be fully applicable to more

advanced phases of ARDS, in whom the magnitude of tidal R/D and association with outcomes could differ. Fourth, although tidal R/D and reversible lung collapse were correlated, their absolute values did not perfectly align in many patients. Because tidal R/D increases compliance even in the absence of stable recruitment (43,46), estimates of recruitability by EIT based on compliance changes could be poorly correlated, especially in spontaneously breathing patients with higher respiratory drive. Also, lung collapse derived from a decremental PEEP trial could underestimate the loos of lung volume occurred after 20 minutes of stable ventilation. Finally, lung morphology was categorized using chest X-rays in nearly half of patients and only two independent reviewers classified the patients, thus the possibility of misclassification cannot be ruled out.

Conclusion

In patients with ARDS undergoing PSV, the magnitude of tidal R/D measured by EIT is highly variable and strongly associated with higher reversible lung collapse, more negative $PL_{End\text{-}Exp}$ values and diffuse distribution of lung infiltrates. Our results may be a step forward towards a better understanding of P-SILI mechanisms, allowing a more precise titration of protective assisted ventilation.

References

1. Slutsky AS, Ranieri VM. Ventilator-Induced Lung Injury. *New England Journal of Medicine* 2013;369:2126–2136.

2. Gaver DP, Kollisch-Singule M, Nieman G, Satalin J, Habashi N, Bates JHT. Mechanical ventilation energy analysis: Recruitment focuses injurious power in the ventilated lung. *Proc Natl Acad Sci U S A* 2025;122:e2419374122.

3. Cressoni M, Cadringher P, Chiurazzi C, Amini M, Gallazzi E, Marino A, *et al.* Lung inhomogeneity in patients with acute respiratory distress syndrome. *Am J Respir Crit Care Med* 2014;189:149–158.

4. Mead J, Takishima T, Leith D. Stress distribution in lungs: a model of pulmonary elasticity. *J Appl Physiol* 1970;28:596–608.

5. Kay SS, Bilek AM, Dee KC, Gaver III DP, Gaver DP. Pressure gradient, not exposure duration, determines the extent of epithelial cell damage in a model of pulmonary airway reopening Downloaded from. *J Appl Physiol* 2004;97:269–276.

6. Bilek AM, Dee KC, Iii DPG, Gaver DP. Mechanisms of surface-tension-induced epithelial cell damage in a model of pulmonary airway reopening. *J Appl Physiol* 2003;94:10.

7. Argiras EP, Blakeley CR, Dunnill MS, Otremski S, Sykes MK. *HIGH PEEP DECREASES HYALINE MEMBRANE FORMATION IN SURFACTANT DEFICIENT LUNGS*. *Br J Anaesth* 1987.

8. Mead J, Takishima T, Leith D. Stress distribution in lungs: a model of pulmonary elasticity. *J Appl Physiol* 1970;28:596–608.

9. Tremblay L, Valenza F, Ribeiro SP, Li J, Slutsky AS. *Injurious Ventilatory Strategies Increase Cytokines and c-fos m-RNA Expression in an Isolated Rat Lung Model*. *J Clin Invest* 1997.

10. Muscedere JG, Mullen JB, Gan K, Slutsky AS. Tidal ventilation at low airway pressures can augment lung injury. *Am J Respir Crit Care Med* 1994;149:1327–34.

11. Liu S, Tan L, Möller K, Frerichs I, Yu T, Liu L, *et al.* Identification of regional overdistension, recruitment and cyclic alveolar collapse with electrical impedance tomography in an experimental ARDS model. *Crit Care* 2016;20:119.

12. Reep CAT, Wils E-J, Fleuren LM, Breskin A, Bellani G, Laffey JG, *et al.* Early versus Delayed Switching from Controlled to Assisted Ventilation: A Target Trial Emulation. *Am J Respir Crit Care Med* 2025;211:975–983.

13. Pérez J, Accoce M, Dorado JH, Gilgado DI, Navarro E, Cardoso GP, *et al.* Failure of First Transition to Pressure Support Ventilation after Spontaneous Awakening Trials in Hypoxemic Respiratory Failure: Influence of COVID-19. *Crit Care Explor* 2023;5:E0968.

14. Perez, Joaquin, Marco Leali, Elena Spinelli, Valentina Chiavieri, Tommaso Rosà, Pierluigi Ferrara, Gaetano Scaramuzzo, Massimo Antonelli, Giacomo Grasselli, Domenico L. Grieco, Savino Spadaro, and Tommaso Mauri. “Physiological Determinants of Tidal Recruitment/Derecruitment Assessed by Electrical Impedance Tomography in Spontaneously Breathing ARDS Patients.” Abstract. Paper presented at the 3rd PLUG Meeting Symposium, Barcelona, 2025.

15. Mauri T, Grieco DL, Spinelli E, Leali M, Perez J, Chiavieri V, *et al.* Personalized positive end-expiratory pressure in spontaneously breathing patients with acute respiratory distress syndrome by simultaneous electrical impedance tomography and transpulmonary pressure monitoring: a randomized crossover trial. *Intensive Care Med* 2024;doi:10.1007/s00134-024-07695-y.

16. Baydur A, Cha E-J, Sassoon CSH. *Validation of esophageal balloon technique t different lung volumes and postures*. 1987. at <www.physiology.org/journal/jappl>.

17. Fumagalli J, Berra L, Zhang C, Pirrone M, Santiago RRDS, Gomes S, *et al.* Transpulmonary pressure describes lung morphology during decremental positive end-expiratory pressure trials in obesity. *Crit Care Med* 2017;45:1374–1381.

18. Nakagawa S, Schielzeth H. A general and simple method for obtaining R^2 from generalized linear mixed-effects models. *Methods Ecol Evol* 2013;4:133–142.

19. Yoshida T, Uchiyama A, Matsuura N, Mashimo T, Fujino Y. The comparison of spontaneous breathing and muscle paralysis in two different severities of experimental lung injury. *Crit Care Med* 2013;41:536–545.

20. Yoshida T, Torsani V, Gomes S, Santis RRD, Beraldo MA, Costa ELV, *et al.* Spontaneous effort causes occult pendelluft during mechanical ventilation. *Am J Respir Crit Care Med* 2013;188:1420–1427.

21. Bassi T, Dianti J, Roman-Sarita G, Bellissimo C, Morris IS, Slutsky AS, *et al.* Effect of Higher or Lower PEEP on Pendelluft During Spontaneous Breathing Efforts in Acute Hypoxemic Respiratory Failure. 2024;doi:10.4187/respcare.12193.

22. Yoshida T, Roldan R, Beraldo MA, Torsani V, Gomes S, De Santis RR, *et al.* Spontaneous effort during mechanical ventilation: Maximal injury with less positive end-expiratory pressure. *Crit Care Med* 2016;44:e678–e688.

23. Morais CCA, Koyama Y, Yoshida T, Plens GM, Gomes S, Lima CAS, *et al.* High positive end-Expiratory pressure renders spontaneous effort noninjurious. *Am J Respir Crit Care Med* 2018;197:1285–1296.

24. Bruhn A, Bugedo D, Riquelme F, Varas J, Retamal J, Besa C, *et al.* Tidal volume is a major determinant of cyclic recruitment-derecruitment in acute respiratory distress syndrome. *Minerva Anestesiol* 2011;77:418–26.

25. Thiese MS, Ronna B, Ott U. P value interpretations and considerations. *J Thorac Dis* 2016;8:E928–E931.

26. Liu H, Wu T. *Estimating the Area under a Receiver Operating Characteristic (ROC) Curve For Repeated Measures Design*.

27. Bertoni M, Telias I, Urner M, Long M, Del Sorbo L, Fan E, *et al.* A novel non-invasive method to detect excessively high respiratory effort and dynamic transpulmonary driving pressure during mechanical ventilation. *Crit Care* 2019;23:.

28. Liu H, Wu T. Estimating the Area Under a Receiver Operating Characteristic Curve For Repeated Measures Design. *J Stat Softw* 2003;8:.

29. Yoshida T, Amato MBP, Kavanagh BP. Understanding spontaneous vs. ventilator breaths: impact and monitoring. *Intensive Care Med* 2018;44:2235–2238.

30. Webb HH, Tierney DF. Experimental pulmonary edema due to intermittent positive pressure ventilation with high inflation pressures. Protection by positive end-expiratory pressure. *Am Rev Respir Dis* 1974;110:556–65.

31. Tremblay L, Valenza F, Ribeiro SP, Li J, Slutsky AS. Injurious ventilatory strategies increase cytokines and c-fos m-RNA expression in an isolated rat lung model. *Journal of Clinical Investigation* 1997;99:944–952.

32. Dreyfuss D, Soler P, Basset G, Saumon G. High Inflation Pressure Pulmonary Edema: Respective Effects of High Airway Pressure, High Tidal Volume, and Positive End-expiratory Pressure. *American Review of Respiratory Disease* 1988;137:1159–1164.

33. Steinberg JM, Schiller HJ, Halter JM, Gatto LA, Lee HM, Pavone LA, *et al.* Alveolar Instability Causes Early Ventilator-induced Lung Injury Independent of Neutrophils. *Am J Respir Crit Care Med* 2004;169:57–63.

34. Tschumperlin DJ, Oswari J, Margulies SS. *Deformation-Induced Injury of Alveolar Epithelial Cells Effect of Frequency, Duration, and Amplitude*. *Am J Respir Crit Care Med* 2000.

35. Crotti S, Mascheroni D, Caironi P, Pelosi P, Ronzoni G, Mondino M, *et al.* Recruitment and derecruitment during acute respiratory failure: a clinical study. *Am J Respir Crit Care Med* 2001;164:131–40.

36. Caironi P, Cressoni M, Chiumello D, Ranieri M, Quintel M, Russo SG, *et al.* Lung opening and closing during ventilation of acute respiratory distress syndrome. *Am J Respir Crit Care Med* 2010;181:578–586.

37. Andrews PL, Sadowitz B, Kollisch-Singule M, Satalin J, Roy S, Snyder K, *et al.* Alveolar instability (atelectrauma) is not identified by arterial oxygenation

predisposing the development of an occult ventilator-induced lung injury. *Intensive Care Medicine Experimental* 2015;3:.

38. Halter JM, Steinberg JM, Gatto LA, DiRocco JD, Pavone LA, Schiller HJ, *et al.* Effect of positive end-expiratory pressure and tidal volume on lung injury induced by alveolar instability. *Crit Care* 2007;11:.
39. Terragni PP, Rosboch G, Tealdi A, Corno E, Menaldo E, Davini O, *et al.* Tidal hyperinflation during low tidal volume ventilation in acute respiratory distress syndrome. *Am J Respir Crit Care Med* 2007;175:160–166.
40. Kiss T, Bluth T, Braune A, Huhle R, Denz A, Herzog M, *et al.* Effects of Positive End-Expiratory Pressure and Spontaneous Breathing Activity on Regional Lung Inflammation in Experimental Acute Respiratory Distress Syndrome. *Crit Care Med* 2019;47:E358–E365.
41. Bassi T, Dianti J, Roman-Sarita G, Bellissimo C, Morris IS, Slutsky AS, *et al.* Effect of Higher or Lower PEEP on Pendelluft During Spontaneous Breathing Efforts in Acute Hypoxemic Respiratory Failure. *Respir Care* 2025;70:126–133.
42. Cressoni M, Chiumello D, Carlesso E, Chiurazzi C, Amini M, Brioni M, *et al.* Compressive forces and computed tomography-derived positive end-expiratory pressure in acute respiratory distress syndrome. *Anesthesiology* 2014;121:572–81.
43. Mojoli F, Pozzi M, Arisi E, Mongodi S, Orlando A, Maggio G, *et al.* Tidal lung hysteresis to interpret PEEP-induced changes in compliance in ARDS patients. *Crit Care* 2023;27:.
44. Mojoli F, Adrião D, Pozzi M, Giacosa M, Couto R, Orlando A, *et al.* Validation of thresholds for tidal lung hysteresis to detect tidal recruitment/derecruitment in ARDS patients. *Am J Respir Crit Care Med* 2026;doi:10.1093/ajrccm/aamaf120.
45. Jonson B, Richard J-C, Straus C, Mancebo J, Lemaire F, Brochard L. *Pressure-Volume Curves and Compliance in Acute Lung Injury Evidence of Recruitment Above the Lower Inflection Point*. *Am J Respir Crit Care Med* 1999.

Figure legends

- **Figure 1.** Graphical representation of tidal recruitment/derecruitment (R/D) measure through electrical impedance tomography (EIT) in four patients ventilated at the two randomized PEEP levels ($PEEP_{EIT}$ and $PEEP_{TABLE}$). The EIT maps were reconstructed at end-expiration (first row) and end-inspiration during tidal ventilation (second row). In the third row, superimposed images of ventilation (dotted white line) and aeration depict regions of tidal R/D in red, defined as areas that were non-aerated at end-expiration but reopened and ventilated during inspiration. Pixels appearing in the image are those with values higher that the thresholds proposed to define aeration (>10%) and ventilation (>30%).

- **Figure 2.** Comparison of tidal recruitment/derecruitment during both randomized PEEP levels ($PEEP_{EIT}$ and $PEEP_{TABLE}$). Points and dotted lines show the individual behavior of each patient. The horizontal and vertical black lines denote the median (25^{th}-75^{th} quantiles) at each randomized PEEP, respectively.

- **Figure 3.** Association between tidal recruitment/derecruitment with end-expiratory transpulmonary pressure (A), reversible lung collapse (B), and morphological distribution of pulmonary infiltrates (C). Black and white dots represent data collected at $PEEP_{TABLE}$ and $PEEP_{EIT}$, respectively. In panel C, the box plots show the median and quantiles 25^{th}-75^{th} (non-focal: 20.7% [11.7–27.9] vs. focal: 4.6% [1.3-12-9]) and white diamonds the mean value (non-focal: 20.8% vs. focal: 8.3%) of tidal recruitment/derecruitment (R/D). Violins represent the density of tidal R/D values across patterns of pulmonary infiltrates distribution.
  Abbreviations: R^2m: marginal determination coefficient; R^2c: conditional determination coefficient.

- **Figure 4.** Forest plot of standardized coefficients (extracted from the final multivariable mixed-effects model) showing the association between end-expiratory transpulmonary pressure ($PL_{End\text{-}Exp;}$ P=0.035), reversible lung collapse (P<0.001) and dynamic driving transpulmonary pressure (ΔPL_{dyn}; P=0.108) with tidal recruitment/derecruitment. The model is adjusted by lung morphology (focal – non-focal), but it has been removed from the plot due to the categorical nature of the variable. Values of standardized coefficients are shown at the right of each diamond to allow comparison between the relative effect size of each one. Variables resulting statistically significant in the adjusted model (P<0.05) are shown with filled black diamond.

- **Figure 5.** Adjusted cumulative incidence of hospital discharge in patients with low and high average tidal recruitment/derecruitment (R/D).
  Abbreviations: HR: hazard ratio.

Figure 1

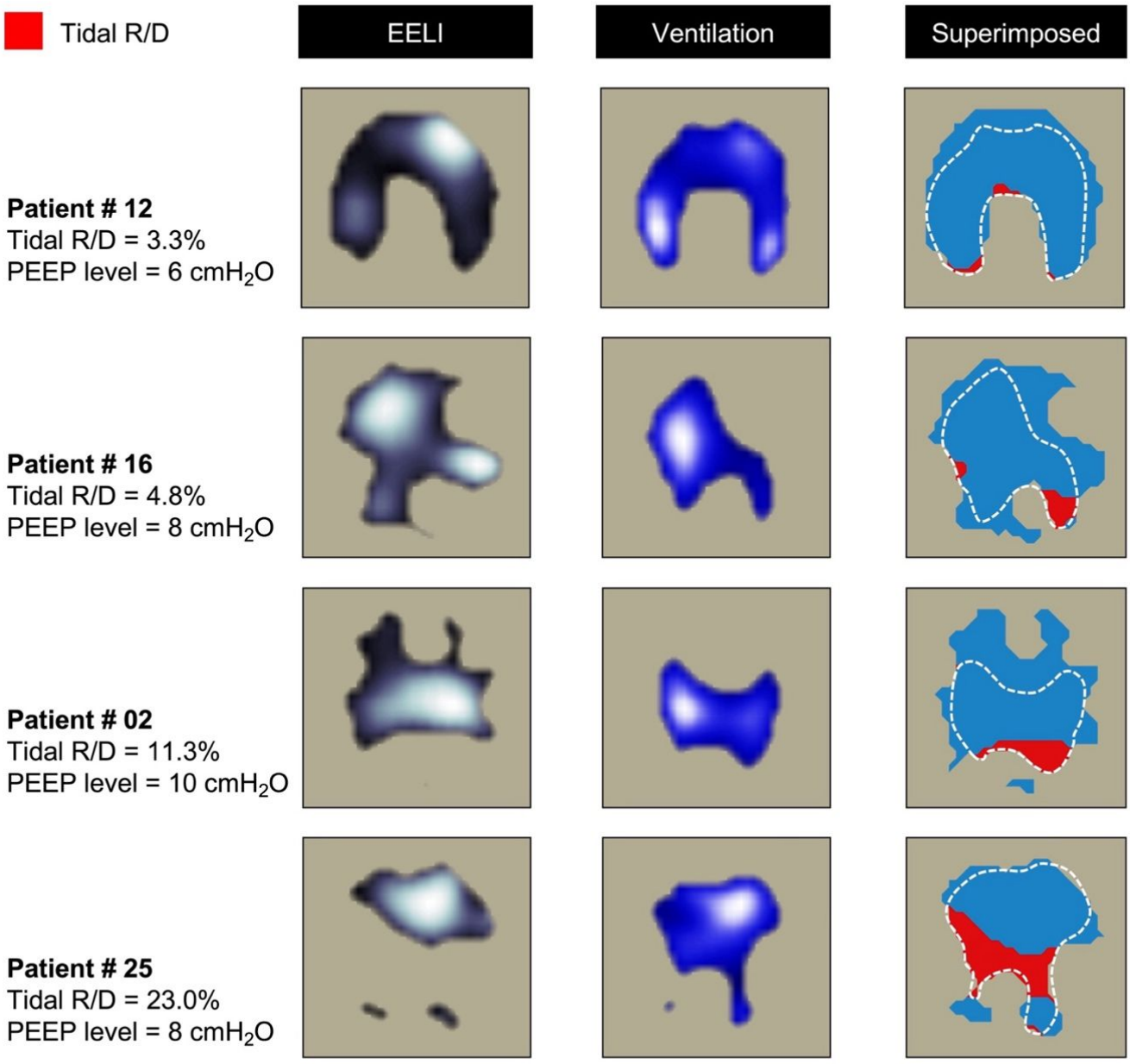

Figure 1. Graphical representation of tidal recruitment/derecruitment (R/D) measure through electrical impedance tomography (EIT) in four patients ventilated at the two randomized PEEP levels ($PEEP_{EIT}$ and $PEEP_{TABLE}$). The EIT maps were reconstructed at end-expiration (first row) and end-inspiration during tidal ventilation (second row). In the third row, superimposed images of ventilation (dotted white line) and aeration depict regions of tidal R/D in red, defined as areas that were non-aerated at end-expiration but reopened and ventilated during inspiration. Pixels appearing in the image are those with values higher that the thresholds proposed to define aeration (>10%) and ventilation (>30%).

Figure 2

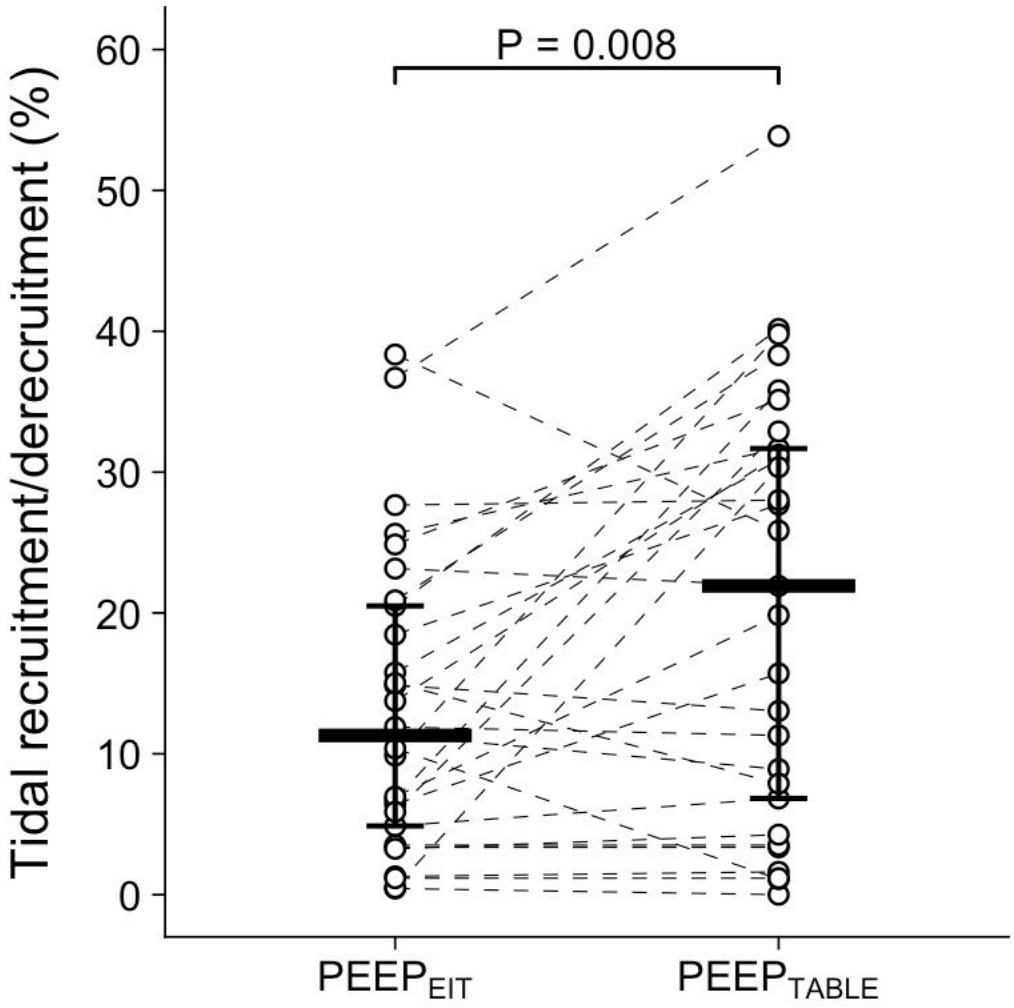

Figure 2. Comparison of tidal recruitment/derecruitment during both randomized PEEP levels ($PEEP_{EIT}$ and $PEEP_{TABLE}$). Points and dotted lines show the individual behavior of each patient. The horizontal and vertical black lines denote the median (25^{th}-75^{th} quantiles) at each randomized PEEP, respectively.

Figure 3

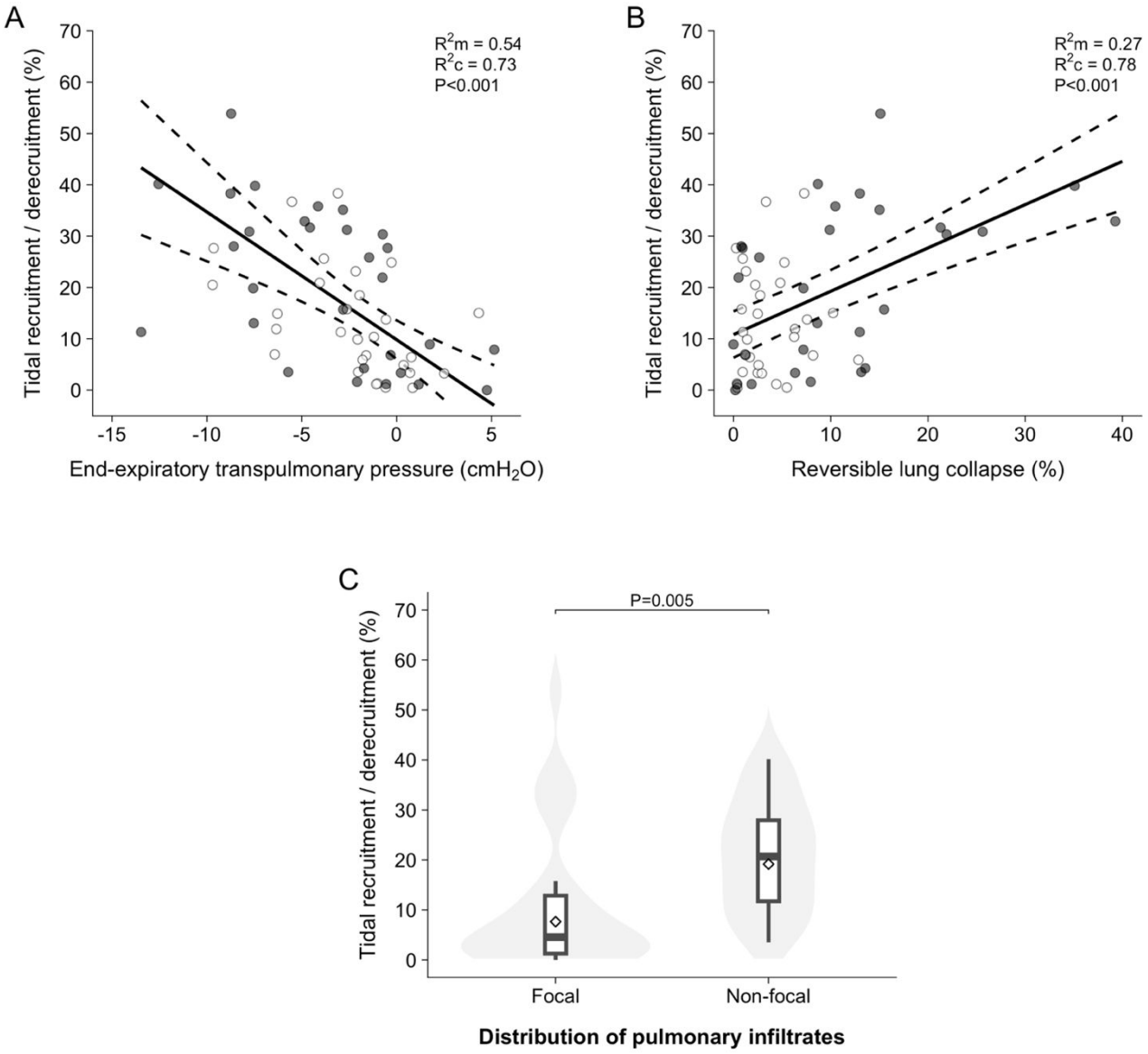

Figure 3. Association between tidal recruitment/derecruitment with end-expiratory transpulmonary pressure (A), reversible lung collapse (B), and morphological distribution of pulmonary infiltrates (C). Black and white dots represent data collected at $PEEP_{TABLE}$ and $PEEP_{EIT}$, respectively. In panel C, the box plots show the median and quantiles 25^{th}-75^{th} (non-focal: 20.7% [11.7–27.9] vs. focal: 4.6% [1.3-12-9]) and white diamonds the mean value (non-focal: 20.8% vs. focal: 8.3%) of tidal recruitment/derecruitment (R/D). Violins represent the density of tidal R/D values across patterns of pulmonary infiltrates distribution.
Abbreviations: R^2m: marginal determination coefficient; R^2c: conditional determination coefficient.

Figure 4

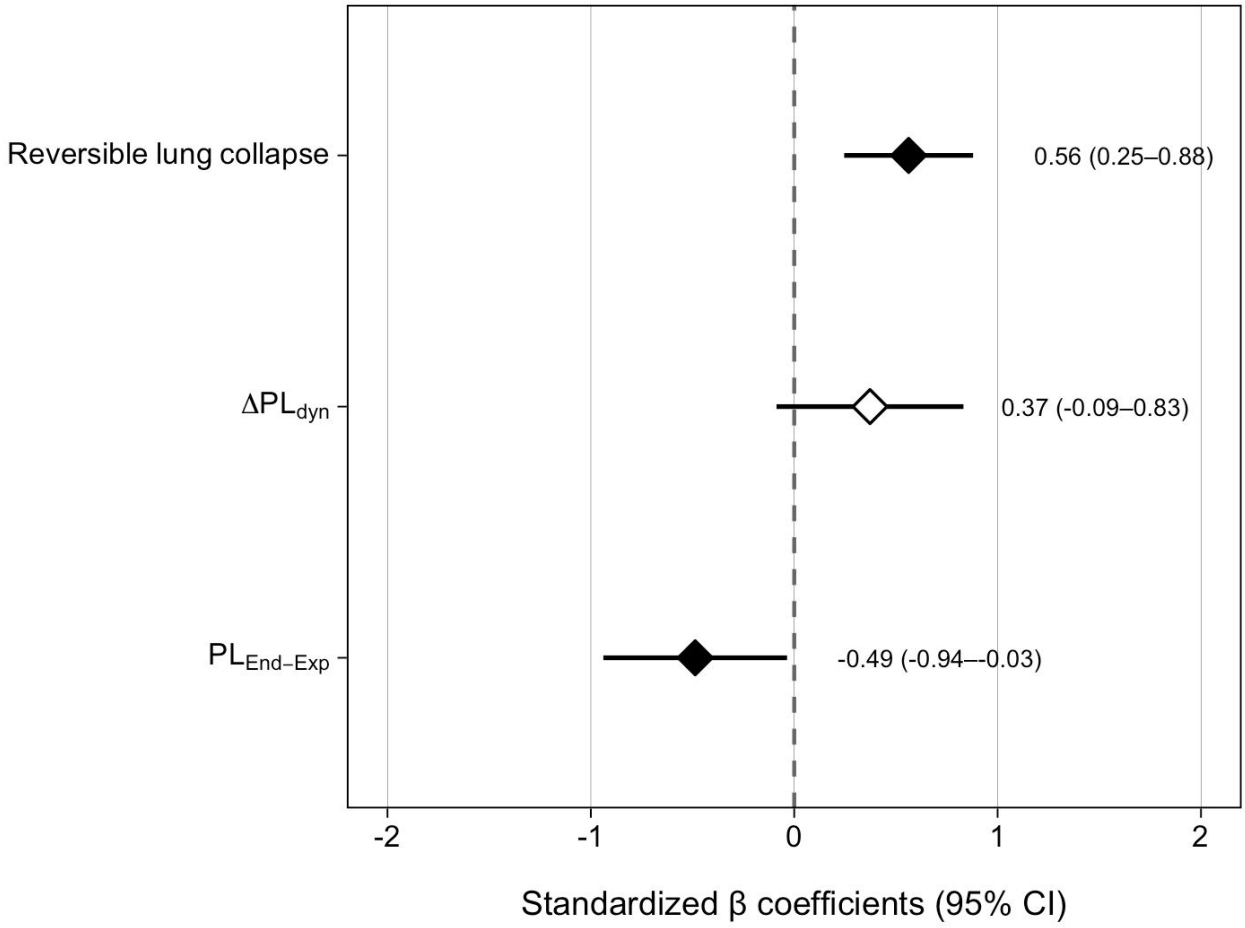

Figure 4. Forest plot of standardized coefficients (extracted from the final multivariable mixed-effects model) showing the association between end-expiratory transpulmonary pressure ($PL_{End-Exp;}$ P=0.035), reversible lung collapse (P<0.001) and dynamic driving transpulmonary pressure (ΔPL_{dyn}; P=0.108) with tidal recruitment/derecruitment. The model is adjusted by lung morphology (focal – non-focal), but it has been removed from the plot due to the categorical nature of the variable. Values of standardized coefficients are shown at the right of each diamond to allow comparison between the relative effect size of each one. Variables resulting statistically significant in the adjusted model (P<0.05) are shown with filled black diamond.

Figure 5

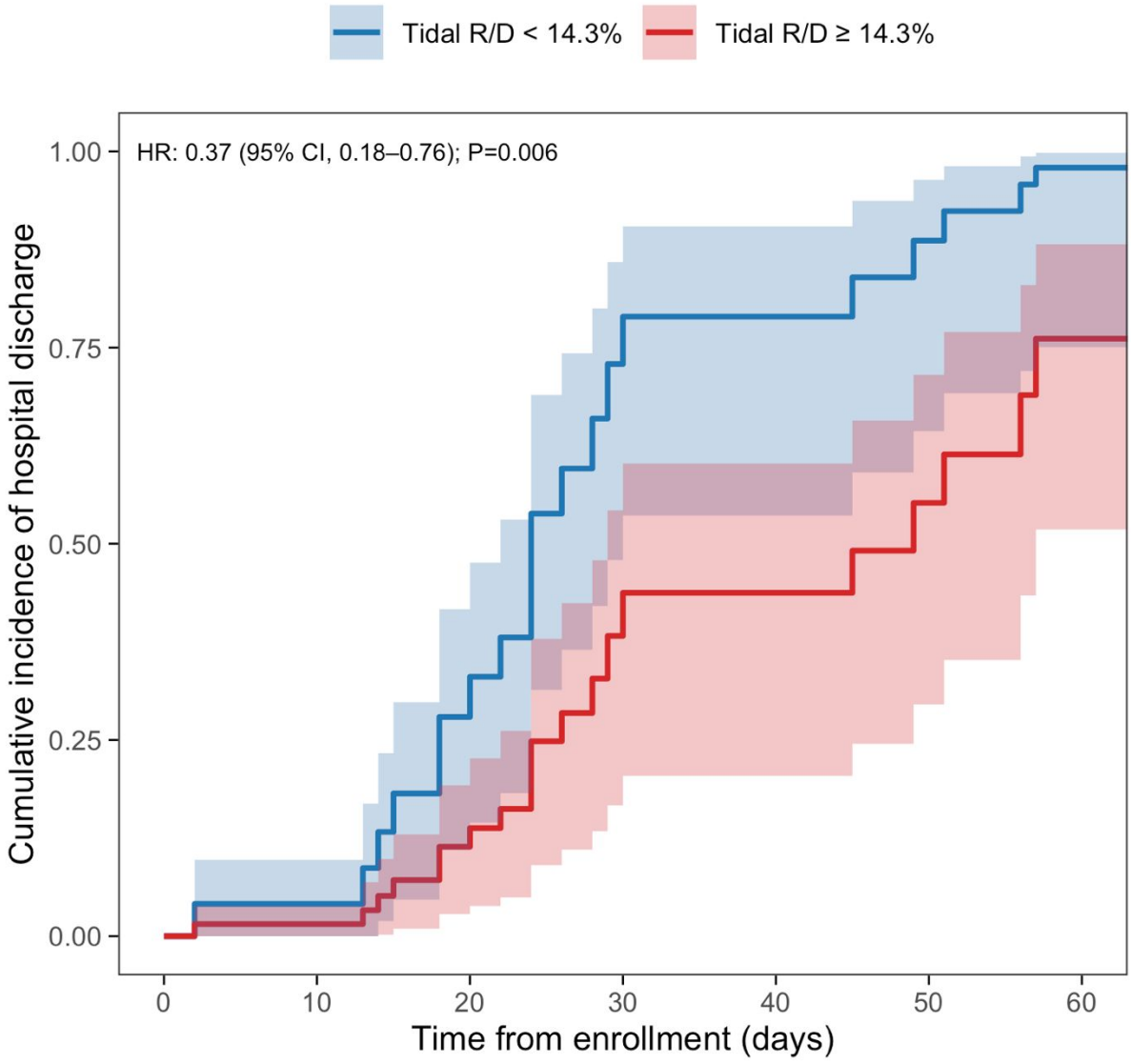

Figure 5. Adjusted cumulative incidence of hospital discharge in patients with low and high average tidal recruitment/derecruitment (R/D). *Abbreviations:* HR: hazard ratio.

Table 1. Characteristics of the patients

Variable	**Value (n = 29)**
• Age (years), mean ± SD	64.0 ± 14.0
• Gender (M/F), n (%)	23 (79.3) / 6 (20.7)
• BMI (Kg/m^2), mean ± SD	27.8 ± 4.9
• SAPS II score at admission, median [Q1-Q3]	41.0 [34.0 – 46.5]
• SOFA (points), median [Q1-Q3]	5.0 [3.0 – 7.0]
Characteristics of ARDS at inclusion	
• Days since intubation, median [Q1-Q3]	6.0 [3.5 – 9.5]
• Days since switch to PSV, median [Q1-Q3]	3.0 [1.0 – 5.0]
• Infectious etiology, n (%)	21 (72.4)
• Primary ARDS, n (%)	22 (75.8)
• Focal / Non-focal ARDS, n (%)	12 (41.4) / 17 (58.6)
• ARDS category (mild/moderate/severe), n (%)	18 (62) / 10 (35) / 1 (3.0)
• Arterial pH, mean ± SD	7.44 ± 0.05
• $PaCO_2$ (mmHg), mean ± SD	45.0 ± 6.3
• PaO_2/FiO_2 (mmHg), mean ± SD	206 ± 54
Outcomes	
• Successful weaning by day 60, n (%)	22 (76)
• ICU length of stay, median [Q1-Q3]	16.0 [12.0 – 28.0]
• Hospital length of stay, median [Q1-Q3]	32.0 [24.0 – 55.0]
• Hospital mortality, n (%)	6 (20.6)

Abbreviations: BMI: body mass index; SAPS: *Simplified Acute Physiology Score*; SOFA: sequential organ failure assessment; PSV: pressure support ventilation; ARDS: acute respiratory distress syndrome;ICU: intensive care unit; $PaCO_2$: arterial pressure of carbon dioxide; PaO_2: arterial pressure of oxygen; FiO_2: fraction of inspired oxygen; SD: standard deviation; Q: quartile.

Table 2. Bivariate associations between tidal recruitment/derecruitment, ventilator settings, monitoring and baseline physiological variables.

Variable	β (95% CI)	R^2m	R^2c	P value
End-expiratory lung inflation and lung compliance				
• PEEP level	−2.24 [−3.09−1.35]	0.17	0.74	**<0.001**
• $PL_{End-Exp}$^	−2.46 [−3.46−1.46]	0.54	0.73	**<0.001**
• Reversible lung collapse^	0.84 [0.57−1.11]	0.27	0.78	**<0.001**
• CL_{dyn}	−0.50 [−0.85−0.15]	0.20	0.73	**0.002**
• Dependent CL_{dyn}	−1.18 [−2.08−0.35]	0.31	0.63	**<0.001**
• Non-dependent CL_{dyn}	−0.45 [−0.89−0.02]	0.09	0.63	**0.048**
Respiratory drive, inspiratory effort and lung stress				
• Plateau pressure	−1.22 [−2.21−0.11]	0.22	0.87	**<0.001**
• Static $PL_{End-Insp}$	−1.60 [−2.58−0.61]	0.29	0.72	**<0.001**
• ΔPL_{dyn}	0.90 [0.20−1.61]	0.15	0.67	**0.009**
• ΔPL_{stat}	1.35 [0.02−0.72]	0.11	0.57	**0.040**
• Pressure support level	0.05 [−1.93−2.06]	0.002	0.57	0.797
• $P_{0.1}$	6.28 [2.80−9.83]	0.33	0.75	**0.001**
• P_{mus}	0.95 [0.29−1.63]	0.14	0.66	**0.009**
• ΔP_{es}	−1.02 [−1.75−0.30]	0.16	0.68	**0.006**
• ΔP_{occ}	−0.56 [−1.15−0.05]	0.15	0.62	**0.035**
• PTP_{mus} per minute	0.08 [0.02−0.14]	0.09	0.66	**0.021**
• ΔP_{es} / ΔPL_{dyn}	0.28 [0.03−0.59]	0.14	0.64	**0.028**
• ΔPL_{dyn} – ΔPL_{stat} difference	0.87 [0.01−1.80]	0.10	0.65	**0.032**
Ventilation heterogeneity and breathing pattern				
• Global inhomogeneity index	0.38 [0.01−0.86]	0.06	0.62	**0.050**
• Local inhomogeneity index	2.06 [0.63−3.49]	0.15	0.61	**0.011**
• Pendelluft magnitude	0.02 [−0.05−0.10]	0.01	0.61	0.462
• Vt/PBW	−0.03 [−2.34−2.19]	0.001	0.56	0.857
• Respiratory rate	0.01 [−0.57−0.61]	0.001	0.57	0.878
• I:E ratio	−3.77 [−20.9−12.9]	0.001	0.55	0.877
Baseline patients characteristics				
• Lung morphology (non-focal)	1.61 [0.57 – 2.65]	0.19	0.57	**0.005**
• PaO_2/FiO_2 > 200 mmHg	0.96 [-023 – 2.16]	0.06	0.57	0.126
• Non-respiratory SOFA	-0.03 [-0.30 – 0.23]	0.02	0.57	0.791
• Body mass index	0.003 [-0.11 – 0.12]	0.001	0.57	0.957
• Static respiratory compliance	-0.03 [-0.01 – 0.04]	0.06	0.63	0.089

^Coefficients are reported with the dependent variable in original scale.
In the remaining variables, the dependet variable was transformed to the square root to reach model's assumptions.
Abbreviations: β: beta coefficient; R^2m: marginal determination coefficient; R^2c: conditional determination coefficient PEEP: positive end-expiratory pressure; ΔPL_{dyn}: dynamic driving transpulmonary pressure; PTP_{mus}: muscular pressure-time product per minute; $PL_{End-Insp}$: end-inspiratory transpulmonary pressure; $PL_{End-Exp}$: end-expiratory transpulmonary pressure; ΔPL_{stat}: static driving transpulmonary pressure; P_{mus}: muscular pressure; $P_{0.1}$: airway oclussion pressure during the first 100 ms; ΔP_{es}: esophageal pressure swing; ΔPocc: airway oclussion pressure; PTP_{mus}: muscular pressure-time product; CL_{dyn}: Dynamic lung compliance; Vt/PBW: tidal volumen adjusted to predicted body weight; I:E: inspiration:expiration; SOFA: sequential organ Failure assessment.

Table 3. Multivariable mixed-effects regression showing independent determinant of tidal recruitment/derecruitment

Variable	β coefficient	95% CI	P value
• $PL_{End-Exp}$	−0.12	-0.22 – -0.02	**0.035**
• Reversible lung collapse	0.07	0.03 – 1.10	**<0.001**
• Lung morphology [non-focal]	1.49	0.61 – 2.36	**0.003**
• ΔPL_{dyn}	0.06	-0.01 – 0.14	0.109

*In the multivariable model, the dependent variable tidal R/D has been transformed to the square-root to achieve model's assumptions. Beta coefficients are expressed in the transformed scale.

Abbreviations: ΔPL_{dyn}: Dynamic driving transpulmonary pressure; $PL_{End-Exp}$: end-expiratory transpulmonary pressure

Table 4. Discriminative power of different thresholds of bedside monitoring variables to identify tidal recruitment/derecruitment ≥ 10.0%

	Cutoff value (cmH_2O)	Sensitivity	Specificity	Youden index	AUC [95% CI]
$PL_{End-Exp}$	-2	0.74	0.78	0.53	0.84 [0.74–0.95]
	-1	0.83	0.57	0.39	-
	0	0.97	0.43	0.41	-
	1	0.97	0.22	0.19	-
	2	0.97	0.13	0.10	-
$P_{0.1}$	2	0,6	0,65	0,25	0.72 [0.58–0.85]
	3	0,31	0,91	0,23	-
	4	0,17	1.00	0,17	-
	5	0,09	1.00	0,09	-
	6	0,06	1.00	0,06	-
ΔPL_{dyn}	15	0.43	0.83	0.25	0.64 [0.49–0.78]
	20	0.26	0.91	0.17	-
	25	0.17	0.96	0.13	-
	30	0.03	1.00	0.03	-
	35	0.00	1.00	0.00	-
P_{mus}	10	0.51	0.65	0.17	0.67 [0.53–0.82]
	15	0.26	0.87	0.13	-
	20	0.14	1.00	0.14	-
	25	0.06	1.00	0.06	-
	30	0.03	1.00	0.03	-

Abbreviations: $PL_{End-Exp}$: end-expiratory transpulmonary pressure; ΔPL_{dyn} : Dynamic driving transpulmonary pressure; P_{mus}: muscular pressure; $P_{0.1}$: airway oclussion pressure during the first 100 ms.

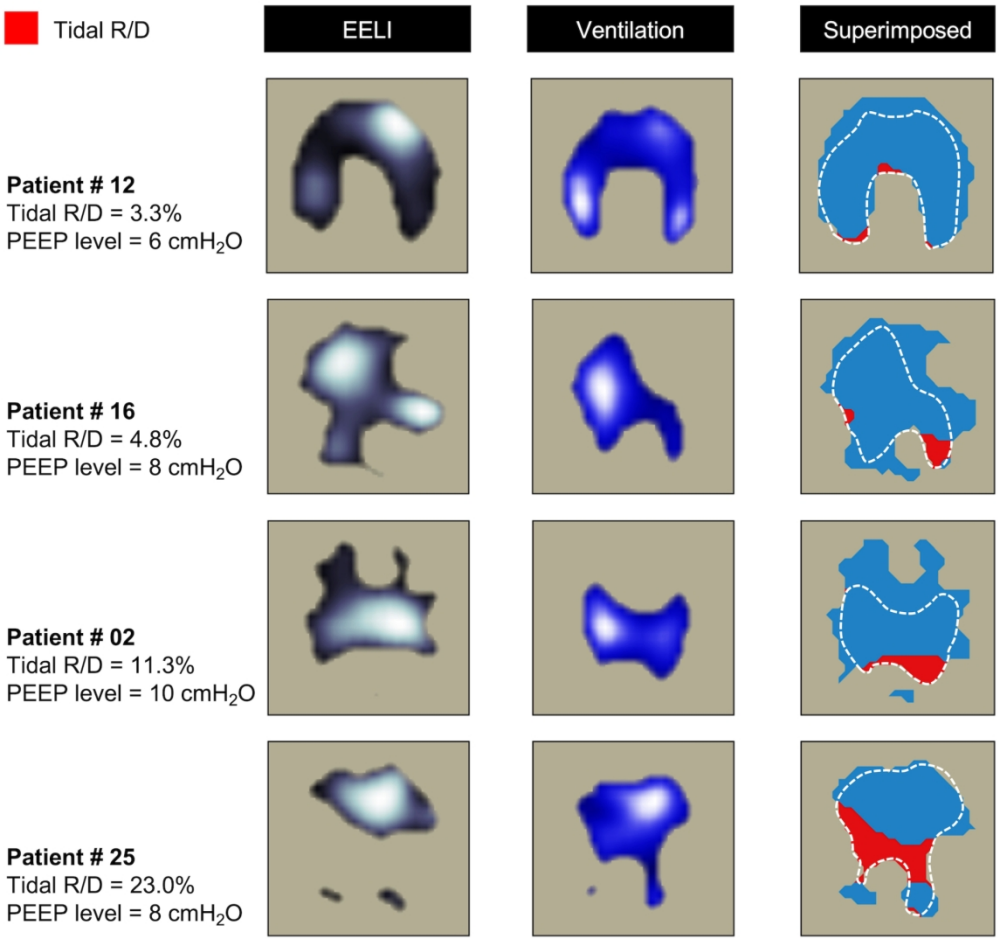

Figure 1. Graphical representation of tidal recruitment/derecruitment (R/D) measure through electrical impedance tomography (EIT) in four patients ventilated at the two randomized PEEP levels (PEEPEIT and PEEPTABLE). The EIT maps were reconstructed at end-expiration (first row) and end-inspiration during tidal ventilation (second row). In the third row, superimposed images of ventilation (dotted white line) and aeration depict regions of tidal R/D in red, defined as areas that were non-aerated at end-expiration but reopened and ventilated during inspiration. Pixels appearing in the image are those with values higher that the thresholds proposed to define aeration (>10%) and ventilation (>30%).

173x162mm (300 x 300 DPI)

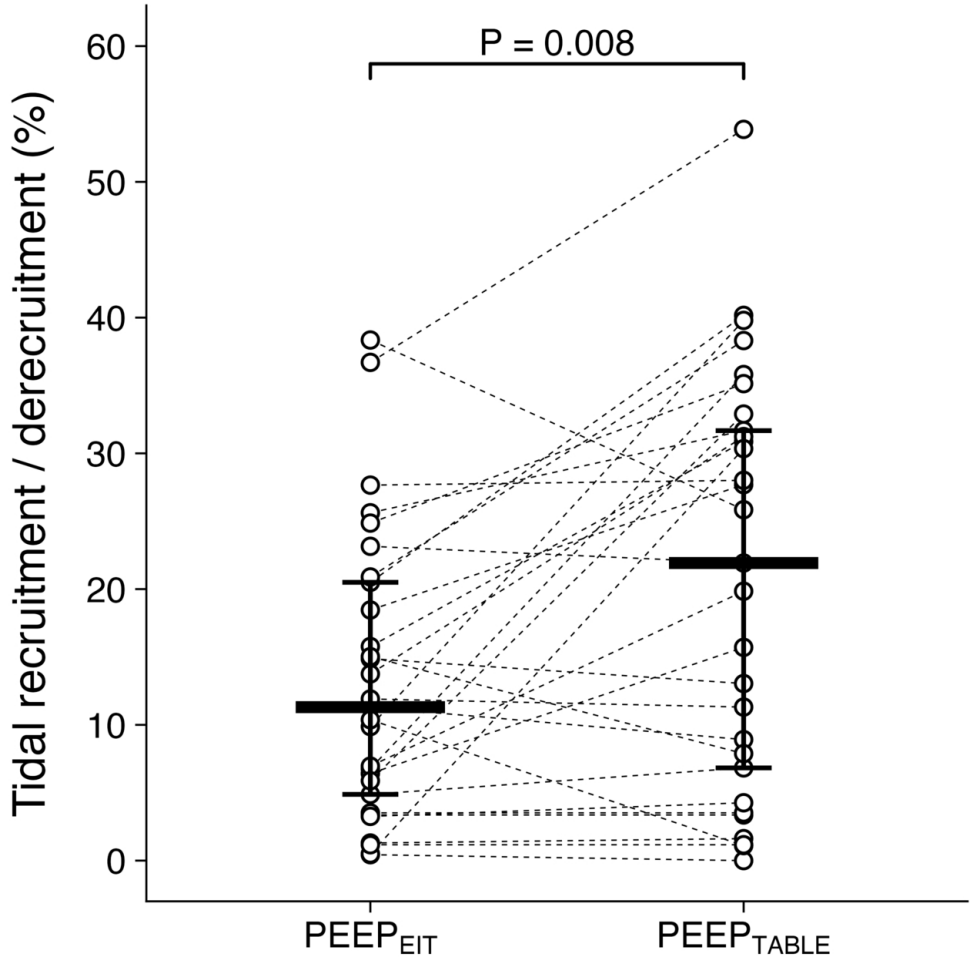

Figure 2. Comparison of tidal recruitment/derecruitment during both randomized PEEP levels (PEEPEIT and PEEPTABLE). Points and dotted lines show the individual behavior of each patient. The horizontal and vertical black lines denote the median (25th-75th quantiles) at each randomized PEEP, respectively.

109x109mm (300 x 300 DPI)

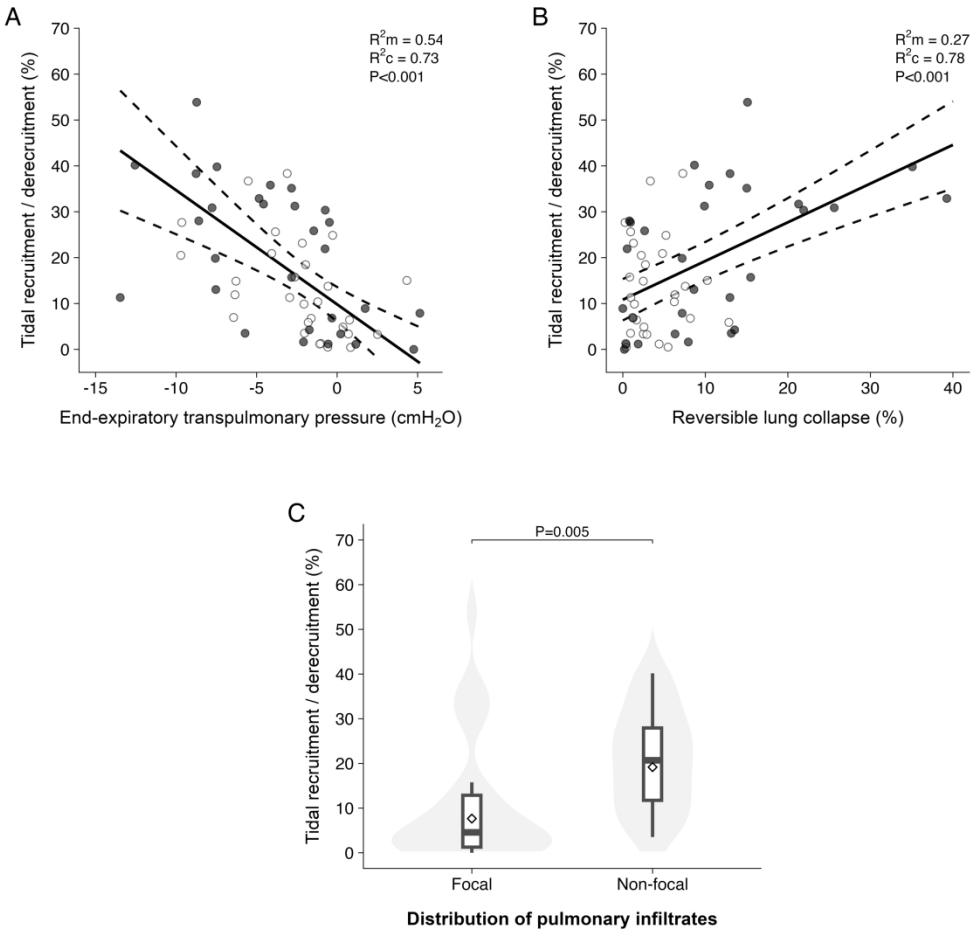

Figure 3. Association between tidal recruitment/derecruitment with end-expiratory transpulmonary pressure (A), reversible lung collapse (B), and morphological distribution of pulmonary infiltrates (C). Black and white dots represent data collected at PEEPTABLE and PEEPEIT, respectively. In panel C, the box plots show the median and quantiles 25th-75th (non-focal: 20.7% [11.7–27.9] vs. focal: 4.6% [1.3-12-9]) and white diamonds the mean value (non-focal: 20.8% vs. focal: 8.3%) of tidal recruitment/derecruitment (R/D). Violins represent the density of tidal R/D values across patterns of pulmonary infiltrates distribution. Abbreviations: R2m: marginal determination coefficient; R2c: conditional determination coefficient.

269x259mm (300 x 300 DPI)

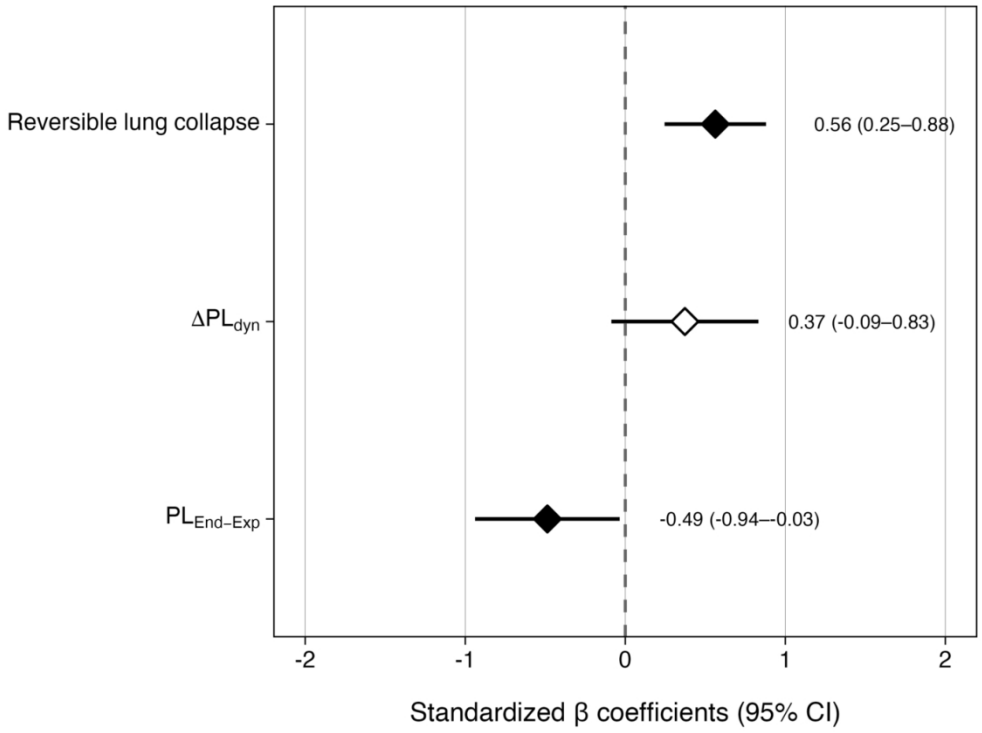

Figure 4. Forest plot of standardized coefficients (extracted from the final multivariable mixed-effects model) showing the association between end-expiratory transpulmonary pressure (PLEnd-Exp; P=0.035), reversible lung collapse (P<0.001) and dynamic driving transpulmonary pressure (ΔPLdyn; P=0.108) with tidal recruitment/derecruitment. The model is adjusted by lung morphology (focal – non-focal), but it has been removed from the plot due to the categorical nature of the variable. Values of standardized coefficients are shown at the right of each diamond to allow comparison between the relative effect size of each one. Variables resulting statistically significant in the adjusted model (P<0.05) are shown with filled black diamond.

119x89mm (300 x 300 DPI)

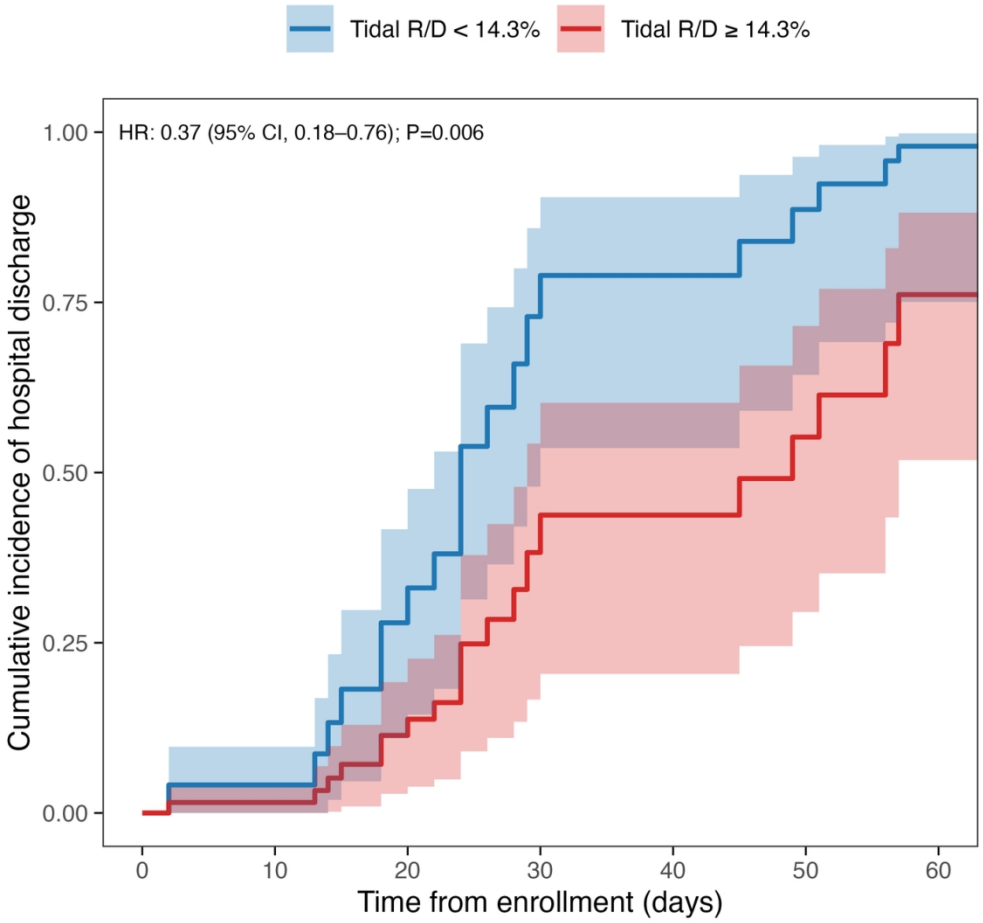

Figure 5. Adjusted cumulative incidence of hospital discharge in patients with low and high average tidal recruitment/derecruitment (R/D).
Abbreviations: HR: hazard ratio.

119x114mm (300 x 300 DPI)